University of Groningen

Graphene and doped graphene from adsorbed molecules

Zehra, Tashfeen

IMPORTANT NOTE: You are advised to consult the publisher's version (publisher's PDF) if you wish to cite from it. Please check the document version below.

Document Version
Publisher's PDF, also known as Version of record

Publication date:
2018

Link to publication in University of Groningen/UMCG research database

Citation for published version (APA):
Zehra, T. (2018). *Graphene and doped graphene from adsorbed molecules*. [Thesis fully internal (DIV), University of Groningen]. University of Groningen.

Copyright
Other than for strictly personal use, it is not permitted to download or to forward/distribute the text or part of it without the consent of the author(s) and/or copyright holder(s), unless the work is under an open content license (like Creative Commons).

The publication may also be distributed here under the terms of Article 25fa of the Dutch Copyright Act, indicated by the "Taverne" license. More information can be found on the University of Groningen website: https://www.rug.nl/library/open-access/self-archiving-pure/taverne-amendment.

Take-down policy
If you believe that this document breaches copyright please contact us providing details, and we will remove access to the work immediately and investigate your claim.

Downloaded from the University of Groningen/UMCG research database (Pure): http://www.rug.nl/research/portal. For technical reasons the number of authors shown on this cover page is limited to 10 maximum.

Download date: 30-11-2023

Chapter 2

Experimental procedures

In this chapter we first describe the growth of graphene on polycrystalline clean copper foils and Cu(111) by Chemical Vapour Deposition (CVD) and then the graphene transfer protocol on Transmission Electron Microscopy grids. CVD grown graphene will be used for comparison with the graphene grown from self-assembled monolayers. Then we illustrate experimental techniques used to characterize graphene and doped graphene synthesized from self-assembled monolayers and adsorbed molecules. The detailed synthesis methods to grow graphene and doped graphene will be explained in Chapters 3 to 6.

2.1 Graphene growth by chemical vapour deposition and transfer protocol

2.1.1 Graphene growth on polycrystalline copper foils by CVD method

Graphene was grown on Cu foil (thickness 25 μm, 99.99% purity, Goodfellow) in a vacuum furnace (base pressure 10^{-5} mbar). Before transfer to the oven the copper surface was etched in 0.25 mM of sulphuric acid (H_2SO_4, Sigma-Aldrich) and rinsed in deionized water (Milli-Q, resistivity 18 GΩcm) to remove the oxide layer from surface. The Cu foil was then annealed in a mixture of 0.5 mbar of hydrogen (Messer, purity 5.0) and 0.1 mbar of argon (Linde, purity 5.0) for 40 minutes. The graphene was grown by exposing the Cu foil to 0.1 mbar of argon, 0.5 mbar of hydrogen and 0.5 mbar of methane (Messer, purity 4.0) for two minutes at 1180 K. The sample was subsequently cooled to room temperature in 0.1mbar argon at a cooling rate of 10 K/min [1].

2.1.2 Graphene growth on Cu(111) by CVD method

The Cu(111) single crystal was cleaned by Ar-sputtering (E_{kin}=1 keV) and annealing in UHV (10^{-10} mbar) at about 700 K. Low Energy Electon Diffraction (LEED) and X-ray Photoelectron Spectroscopy (XPS) were used to check the cleanliness of the sample surface. The single crystal was then transferred to the CVD oven. During transfer through the air, a layer of copper oxide and carbon contaminations was formed on surface. To remove contaminations and reduce the oxide the sample was annealed in 0.1 mbar argon (Linde, purity 5.0) and 0.5 mbar hydrogen flow (Messer, purity 5.0) at 1200 K for four hours. Subsequently the graphene was grown by exposing the Cu(111) crystal to 0.1 mbar argon, 0.5 mbar hydrogen and 0.5

mbar methane for 3-4 minutes; the sample was then annealed in 0.1 mbar argon and 0.5 mbar hydrogen for 30 min before being cooled down in 0.1 mbar argon at a cooling rate of 5 K/min [2].

2.1.3 Transfer of graphene onto TEM grids

The growth of good quality graphene from self-assembled monolayers on copper substrates can open the possibility to transfer it to other substrates of choice to conduct further studies of the material. We transferred the graphene grown on clean/oxidized copper foils onto Quantifoil®2/2 Transmission Electron Microscopy (TEM) grids (Quantifoil Micro Tools GmbH). As shown in figure 2.1, these grids consists of 100 μm spaced Au-mesh onto which an amorphous carbon membrane of 12 nm thickness has been deposited. This membrane contains 2 μm diameter circular holes with a spacing of 2 μm.

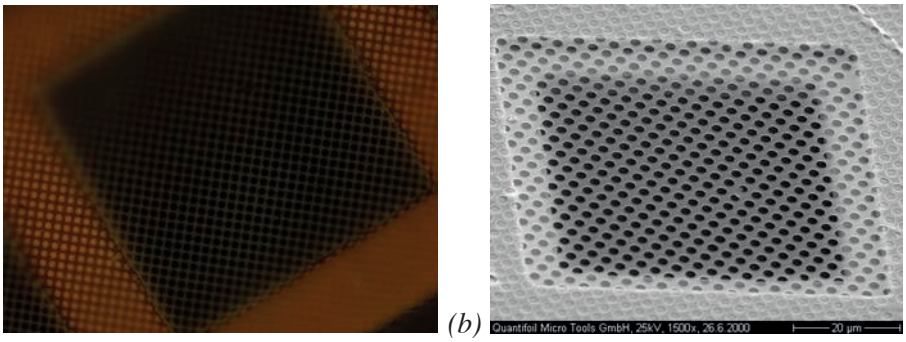

Figure 2.1: *(a) Optical microscope image and (b) SEM image of a Quantifoil®2/2 on gold TEM grid. Image (b) from http://www.quantifoil.com*

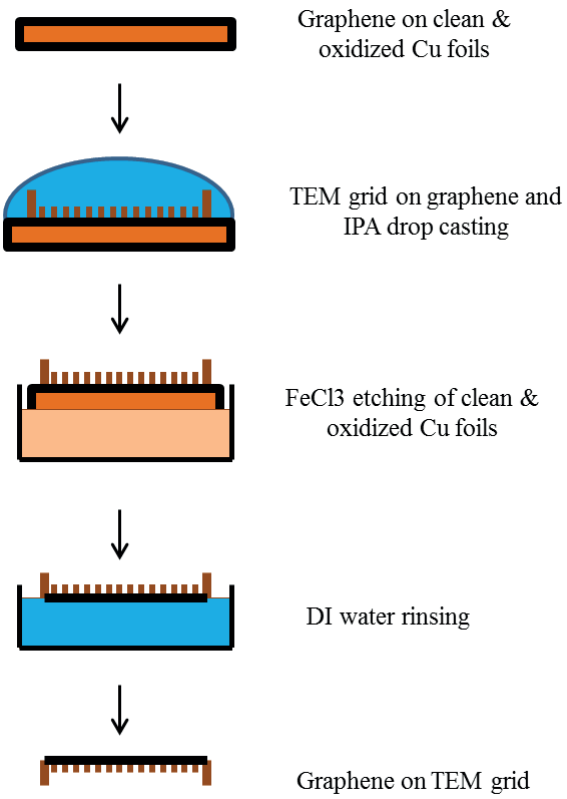

Figure 2.2: *Procedure to transfer graphene from clean and oxidized copper foils to TEM grids. Taken from [3]*

Free standing graphene, free of residues and impurities, was prepared on TEM grids by following procedure described in [3] and shown in figure 2.2. The Quantifoil®2/2 TEM grid was directly placed on the copper foil with amorphous carbon membrane in contact with graphene. A drop of 2-propanol alcohol (IPA, 99.95% purity, Merck) was deposited onto the graphene. During evaporation of the IPA, graphene and amorphous carbon membrane attached to one another. The sample was then placed in a 5 mM solution of $FeCl_3$ (99.99 %, Sigma-Aldrich) in water to etch away the copper foil. The TEM grid with the graphene was then thoroughly rinsed three times

with ultrapure deionized water (Milli-Q, resistivity 18 GΩcm). The graphene on the TEM grid was then annealed at 400 K for 5 min in an oven (UNE 200, Memmert) to remove the excess water. Before performing transmission electron microscopy to determine the structural properties, a scanning electron microscope was employed to determine the coverage of the grids (see Chapter 3).

2.2 Characterization techniques

2.2.1 X-ray photoemission spectroscopy

X-ray photoelectron spectroscopy (XPS) was used to investigate the chemical nature of the samples [4]. The technique is also known as electron spectroscopy for chemical analysis (ESCA) and was first employed by Steinhardt and Siegbahn in 1950 [5,6]. In 1981 Kai Siegbahn was awarded with the Nobel Prize for his contribution to the development of the theory and the instrumentation of XPS. Nowadays XPS has become a standard surface science technique to determine the surface stoichiometry and gaining insight into the type of bonds formed by the surface atoms. XPS is based on photoelectric effect. When the surface of a material is irradiated with photons having sufficient energy ($h\nu$), electrons are emitted. In XPS the kinetic energies of electrons emitted from core levels, E'_k , are analysed. E'_k is given by the following equation and illustrated in figure 2.3:

$$E'_k = h\nu - E_b - \Phi_{sp} \qquad 2.1$$

where E_b is the binding energy of the ejected electrons, defined as the energy difference between the initial state (ground state), E_i, and the final

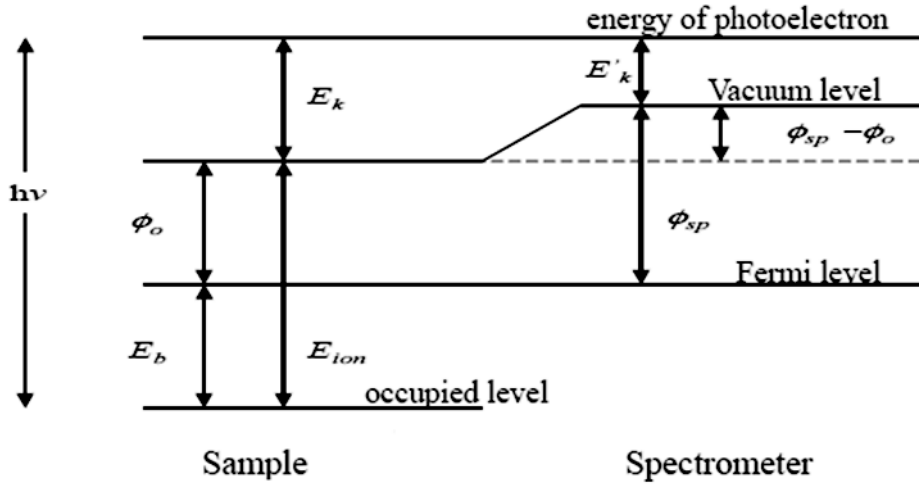

$$h\nu = E_b + E_k + \phi_0$$

$$E_b = E_f - E_i = h\nu - E'_k - \phi_{sp}$$

Figure 2.3: *Schematics of the energy levels involved in X-ray photoelectron spectroscopy when sample and spectrometer are in electrical contact and hence their Fermi levels are aligned (from P. Rudolf's lecture notes on XPS).*

state with a core hole on the surface atom and the free electron, E_f, and Φ_{sp} is the work function of the spectrometer. The binding energy of a certain core level is an intrinsic element specific property; it is influenced by various factors, namely the chemical environment, oxidation/valence and spin states of the atom from which the photoelectron is emitted.

XPS not only gives the information about the elemental composition of the surface but we can also use it to determine the chemical environment of each constituent element. The oxidation and spin states of the atoms at the

surface of material can be determined very accurately by this technique. The penetration depth of the incident X-rays photons for a given material is quite large. However, for a laboratory source, the electron mean free path of the photoelectrons is very small - typically of the order of few nm - due to inelastic scattering. Hence, only those photoelectrons coming from first few atomic layers will escape without scattering. This explains the surface sensitivity of the XPS technique.

For the studies described in this dissertation, XPS spectra were collected by employing a monochromatic Al K_α X-ray source ($h\nu$=1486.6 eV) and a hemispherical electron analyser (Scienta R4000). The spectra of the C1*s*, O1*s*, N1*s*, B1*s*, Cu2$p_{3/2}$ and S2*p* core level regions were acquired at a base pressure of ~9×10^{-10} mbar. The overall experimental resolution was 0.35 eV. XPS spectra were analysed using the least squares curve fitting program Winspec developed at the LISE, University of Namur, Belgium. It includes a Shirley or linear baseline subtraction and a peak deconvolution using a linear combination of Gaussian and Lorentzian functions, taking into account the experimental resolution. The spectra were fitted with a minimum number of peaks consistent with the structure of the molecules on the surface. Binding energies of isolated peaks are given ± 0.05 eV; when more than one component was needed to reproduce the raw data, the error in peak position was ± 0.1 eV. The uncertainties in the intensity determinations were C1*s* 3 %, O1*s* 2.4 %, N1*s* 1.7%, B1*s* 2.3 %, Cu2$p_{3/2}$ 4 % and S2*p* 3.1 %. All measurements were taken on freshly prepared samples; three samples were measured in each case to check for reproducibility.

2.2.2 Raman spectroscopy

Raman spectroscopy is used to detect vibrational, rotational and other low-frequency modes in a sample by exciting it with monochromatic light, usually from a laser source. In Raman most emitted light is scattered elastically, the so-called Rayleigh scattering, having hence the same frequency as the excitation source. A small amount of the scattered light (*ca*. 5-10 % of the incident light intensity) is shifted in energy from the laser frequency due to interactions between the incident electromagnetic waves and the vibrational energy levels of the molecules in the sample. Plotting the intensity of the light versus shifted frequency results in a Raman spectrum with the Rayleigh band at 0 cm^{-1}. The peak positions in the spectra will lie at frequencies that correspond to the vibrations of different functional groups of the sample.

The Raman spectra in the range of 500-3000 cm^{-1} were collected with an Olympus BX51 microscope fiber-coupled to an Andor Technology DU416A-LDC-DD camera coupled to a Shamrock163 spectrograph and 500 l/mm grating blazed at 750 nm. Excitation is with a 632.8 nm HeNe laser (Thorlabs, random polarisation), 9 mW at sample. The spot size diameter is estimated at 1.0 μm with a 100× objective (9 mW, 2 μm spot size with a 50x objective). Each spectrum was the average of 40 scans collected with an estimated 4 cm^{-1} resolution.

2.2.3 Transmission electron microscopy

A transmission electron microscopy operates on the same basic principles as the light microscope but uses a beam of electrons transmitted through a

specimen to form an image. Using electrons as "light source", their much lower wavelength makes it possible to get a much better resolution than with a light microscope. Objects down to atomic dimensions can be imaged with TEM, making it a valuable tool in medical, biological and materials research.

In TEM, electrons emitted from a cathode or a field emission source travel through vacuum in the column of the microscope, where a focused beam is formed with the help of electromagnetic lenses. The electron beam then travels through the specimen of interest. Depending on the density of the material present, some of the electrons are scattered and disappear from the beam. At the bottom of the microscope the unscattered electrons hit a fluorescent screen, which gives rise to a "shadow image" of the specimen with its different parts displayed in varied darkness according to their density. The image can be studied directly by the operator or photographed with a camera, typically a charge-coupled device (CCD).

TEM images were acquired with a JEOL 2010F TEM, equipped with a field emission gun and operated at 200 keV. TEM images in bright field mode and diffraction patterns were collected with a Gatan CCD camera (camera length of 200 mm).

2.2.4 Scanning electron microscopy

A scanning electron microscope (SEM) uses a focused beam of electrons to produce images of a sample by scanning it. The electrons interact with atoms in the sample, yielding different signals that contain information about the sample's surface topography and composition. Samples are

analysed in vacuum and have to be conducting to prevent charging by the electron beam. The usual SEM mode consists in detecting the secondary electrons that are emitted by atoms excited by the electron beam. The number of secondary electrons emitted from a certain spot depends on the sample topography, for example asperities on the surface give rise to an enhanced signal. By scanning the sample and collecting the emitted secondary electrons in every point, a topographic image of the surface is produced.

SEM analysis was performed using a JEOL JSM-7000F microscope equipped with a field emission source operated at 5 kV. Other SEM images (suspended graphene on TEM grids) were collected using a Philips XL30S microscope equipped with a field emission source operated at 5 kV.

2.2.5 Contact angle measurements

The angle a liquid creates with a solid surface when both materials come in contact with each other is called the contact angle; it is a measure of the wettability of a solid by a liquid. The angle depends on properties of the solid and the liquid, the cohesion and adhesion forces between them and by interface properties of the different phases in contact (gas, liquid and solid). At a certain temperature and pressure, a system has a unique equilibrium contact angle. The equilibrium contact angle reflects the relative strength of the liquid/solid, liquid/vapour and solid/vapour molecular interactions and can be calculated by using Young's equation:

$$\gamma_{SG} - \gamma_{SL} - \gamma_{LG} - \cos\theta_C = 0 \qquad 2.2$$

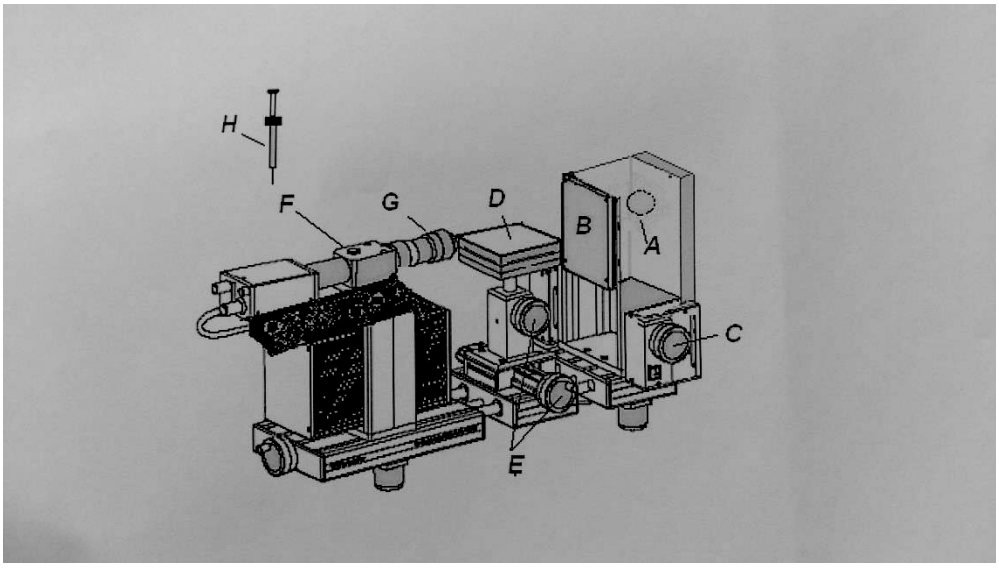

Fig.2.4: *Schematics of apparatus used for contact angle measurements (home built apparatus drawing, Surfaces and Thin Films group, Zernike Institute for Advanced Materials)*

where, γ_{SG} is the solid–vapour interfacial energy, γ_{SL} the solid–liquid interfacial energy, γ_{LG} the liquid–vapor interfacial energy and θ_C the equilibrium contact angle.

The contact angle measurements were carried out with a microscope-goniometer setup connected to a personal computer; both the microscope-goniometer setup and the software (angleanalyse) to calculate the contact angle were built in the Surfaces and Thin Films group. The goniometer is equipped with (A) a source of white light, 5 W lumiLED, (C) with regulation of the light intensity, (B) a frosted Plexiglas light diffuser, (D) the table, (E) with regulation of height and position, (F) and horizontally

mounted monochrome type IEEE 1394 camera, (G) with a 640×480 resolution and a zoom lens with the par focal zoom varying from 0.75× up to 3× (it can be changed by turning the end of the camera G), (H) a Hamilton 25 μl syringe was used to deposit the drops of liquids.

A 2 μl drop of doubly distilled deionized water was used as the measuring liquid (sessile drop method) [7]. Minimum 5 to 7 spots on each sample were measured and the contact angle averaged. Analysis was done by applying a baseline and an elliptical curve fitting of the water-air contact profile. The uncertainty in the measurements is ± 2^{o}.

2.2.6 Low energy electron diffraction (LEED)

Low-energy electron diffraction (LEED) is used to determine the surface structure of single-crystalline materials. A collimated beam of low energy electrons (20–200 eV) is directed at 90^{o} towards the surface of the sample and the diffracted electrons are observed as spots on a fluorescent screen. The analysis of spot positions in diffraction pattern provides information about symmetry of the surface structure. The size and rotational alignment of the adsorbate unit cell with respect to the substrate unit cell can also be calculated.

The low energy electron diffraction patterns were collected with a Specs Omicron ErLEED100/150 system with an ErLEED 1000A analogue power supply. With the ErLEED 1000A the primary energy of the electron is variable from 0-1000 eV.

2.2.7 VUV-Discharge lamp

A gas discharge lamp produces light by generating an electrical discharge through an ionized gas. When a high voltage is applied, an electrical field is generated in the tube that accelerates free electrons in the gas. These electrons collide with the gas atoms exciting electrons to higher energy levels. When these electrons drop back to their previous energy state, energy is released in the form of photons. As discussed in Chapters 3 and 4, the self-assembled monolayers (SAMs) were polymerized by irradiation with an Omicron Focus VUV-Discharge lamp (HIS-13). This is a windowless gas discharge light source for the production of VUV light under vacuum conditions. It can be operated with various discharge gases, such as helium, neon, argon, krypton, xenon or hydrogen. For irradiation of our SAMs we operated with helium in the He I mode at 21.2 eV (584 nm).

References

[1] Bignardi L, Dorp W F Van, Gottardi S, Ivashenko O, Dudin P, Barinov A, De Hosson J T M, Stöhr M and Rudolf P 2013 Microscopic characterisation of suspended graphene grown by chemical vapour deposition. *Nanoscale*. 5 9057–9061

[2] Gottardi S, Müller K, Bignardi L, Moreno-lópez J C, Anh T, Ivashenko O, Yablonskikh M, Barinov A, Björk J, Rudolf P and Stöhr M 2015 Comparing graphene growth on Cu(111) versus oxidized Cu(111) *Nano Lett*. **15** 1–13

[3] Regan W, Alem N, Alemán B, Geng B, Girit Ç, Maserati L, Wang F, Crommie M and Zettl A 2010 A direct transfer of layer-area graphene *Appl. Phys. Lett*. 96 2008–2011

[4] Vickerman J C and Gilmore I 1997 Surface Analysis: the Principal Techniques; (Wiley Online Library)

[5] Steinhardt R and Serfass E 1951 Analytical chemistry: Introduction **23** 308-360

[6] Siegbahn K and Edvarson K 1956 β-ray spectroscopy in the precision range of 1 : 10^5 *Nuclear Physics* **1** 137-159

[7] Mittal K L (ed.) 2003 Contact Angle, wettability and adhesion (VSP Utrecht)